

Efficient transition path sampling: Application to Lennard-Jones cluster rearrangements

Christoph Dellago, Peter G. Bolhuis, and David Chandler

Department of Chemistry, University of California at Berkeley, Berkeley, California 94720

(Received 17 February 1998; accepted 5 March 1998)

We develop an efficient Monte-Carlo algorithm to sample an ensemble of stochastic transition paths between stable states. In our description, paths are represented by chains of states linked by Markovian transition probabilities. Rate constants and mechanisms characterizing the transition may be determined from the path ensemble. We have previously devised several algorithms for sampling the path ensemble. For these algorithms, the numerical effort scales with the square of the path length. In the new simulation scheme, the required computation scales linearly with the length of the transition path. This improved efficiency allows the calculation of rate constants in complex molecular systems. As an example, we study rearrangement processes in a cluster consisting of seven Lennard-Jones particles in two dimensions. Using a quenching technique we are able to identify the relevant transition mechanisms and to locate the related transition states. We furthermore calculate transition rate constants for various isomerization processes. © 1998 American Institute of Physics. [S0021-9606(98)51322-0]

I. INTRODUCTION

Studying transitions between stable states separated by unknown dynamical bottlenecks presents well known computational difficulties. Such transitions are rare events. Conventional methods for studying rare events in many body systems are based on transition state theory. First, one estimates the probability of visiting the dynamical bottleneck—the transition state(s). Then the transmission coefficient and rate constant can be determined from a series of short trajectories initiated from the ensemble of states prepared at that bottleneck.¹⁻⁴ The difficulty with this method is that it requires prior knowledge of the transition states. Without knowledge of the transition states, i.e., without an *a priori* conception of the mechanism or pathway for the process, this approach cannot be applied.

We have recently developed a general computational method capable of circumventing this problem by sampling transition pathways.⁵ Our general approach builds on Pratt's suggestion⁶ for studying the statistics of pathways between two distinct stable states. It requires the specification of dynamical variables called "order parameters" that characterize the stable states but not prior knowledge of transition states. Transition paths are represented by chains of states coupled by Markovian transition probabilities and forced to connect the stable states by suitable constraints. The statistics of such paths is then isomorphic to that of constrained polymers—each degree of freedom maps onto a chain, where successive polymer units represent the degree of freedom at successive time slices.

Transition probabilities determine the links in these chains. The probabilistic nature of the transition paths follows from the specifications of initial and final conditions, and also the type of dynamics. The transition probabilities have to be consistent with the underlying physical process.

For sufficiently simple systems or short enough transition paths, application of the sampling algorithms developed in Ref. 5 is possible.⁷ For many particle systems of modest to high complexity, however, their practicality remains an issue. This paper addresses this issue. We derive a class of algorithms, called "shooting," that scale linearly with path length. As such, the generation of N statistically independent transition paths, each one being L time steps long, requires the same order of computational effort as a straightforward trajectory NL time steps long. But while straightforward trajectories encounter few if any rare events, transition path sampling focuses entirely on the rare events of interest. In this paper, we demonstrate the use of the shooting algorithms with stochastic dynamics. The algorithms are equally applicable, however, to conservative deterministic equations of motion.⁸ Thus, the procedure described in this paper provides the general solution to the problem of computing the rates and correlation functions for rare events in any system for which straightforward numerical simulation is possible.

In Sec. II, we define the "transition path ensemble" and the probability distribution for that ensemble when the dynamics flows according to a Langevin equation of motion. Shooting algorithms are presented in Sec. III. Methods for computing rate constants and related correlation functions from path sampling are discussed in Sec. IV. In Sec. V, the methods are demonstrated by studying rearrangement processes in a two dimensional cluster of seven Lennard-Jones disks. There, a technique we call "path quenching" is used to help identify different reaction mechanisms. We calculate reaction rates for several selected mechanisms. We conclude in Sec. VI with a brief summary of what we have accomplished.

II. THEORETICAL BACKGROUND

A. Transition path action

We describe a stochastic process by a chain of states $\{x\} \equiv \{x_0 \rightarrow x_1 \rightarrow \dots \rightarrow x_L\}$, where x_τ is the point in phase space representing the system at time $t = \tau \Delta t$. The integer subscript τ numbers the states, or time slices, along the chain, and Δt is the time interval between the slices. If consecutive states are linked by a Markovian transition probability $p(x_\tau \rightarrow x_{\tau+1})$, the probability of realizing a particular path is

$$\rho(x_0) \prod_{\tau=0}^{L-1} p(x_\tau \rightarrow x_{\tau+1}), \quad (1)$$

where $\rho(x_0)$ is the distribution of the initial conditions x_0 . For a canonical distribution of initial points $\rho(x_0) = \exp\{-\beta H(x_0)\}$, where $\beta = 1/k_B T$ is the reciprocal temperature and $H(x_\tau)$ is the Hamiltonian of the system at time τ .

To sample the ensemble of transition paths it is convenient to define a path action $S_{AB}[\{x\}]$ including endpoint constraints $h_A(x_0)$ and $h_B(x_L)$ in the path probability

$$\exp(-S_{AB}[\{x\}]) \equiv h_A(x_0) e^{-\beta H(x_0)} \left[\prod_{\tau=0}^{L-1} p(x_\tau \rightarrow x_{\tau+1}) \right] h_B(x_L). \quad (2)$$

The path is forced to start in region A (the reactant region) and to end in region B (the product region) by the characteristic functions

$$h_{A,B}(x) = \begin{cases} 1, & \text{if } x \in A, B, \\ 0, & \text{if } x \notin A, B. \end{cases} \quad (3)$$

As we will show later, in some cases it is appropriate to relax the requirement that the last time slice of the path must be in the product region B . Instead one requires the system to visit region B at some time slice between $\tau=0$ and $\tau=L$ but allows the system to leave B again. In this case, the action \tilde{S}_{AB} of the path is given by

$$\exp(-\tilde{S}_{AB}[\{x\}]) \equiv h_A(x_0) e^{-\beta H(x_0)} \left[\prod_{\tau=0}^{L-1} p(x_\tau \rightarrow x_{\tau+1}) \right] \tilde{h}_B[\{x\}], \quad (4)$$

where $\tilde{h}_B[\{x\}] = 1$ if at least one time slice lies in B and $\tilde{h}_B[\{x\}] = 0$ otherwise.

B. Stochastic dynamics

In this paper, we consider classical many-body systems evolving according to the Langevin equation of motion

$$\begin{aligned} \dot{r} &= v, \\ \dot{v} &= \frac{F(r)}{m} - \gamma v + \frac{\mathcal{R}}{m}. \end{aligned} \quad (5)$$

The positions and velocities of all particles are specified by r and v , respectively. F is the intermolecular force derived from the potential $V(r)$, and γ is a friction constant. The

random force, \mathcal{R} , is responsible for the stochastic character of the time evolution. It is a Gaussian random variable with $\langle \mathcal{R}(t) \mathcal{R}(0) \rangle = 2m\gamma k_B T \delta(t)$. For a short time increment, Δt , the assumption of a force which depends linearly on r leads to the integration algorithm⁹

$$r_{\tau+1} = r_\tau + c_1 \Delta t v_\tau + c_2 \Delta t^2 a_\tau + \delta r_R, \quad (6)$$

$$v_{\tau+1} = c_0 v_\tau + (c_1 - c_2) \Delta t a_\tau + c_2 \Delta t a_{\tau+1} + \delta v_R,$$

where $a_\tau = F(r_\tau)/m$ and the coefficients c_0 , c_1 and c_2 are given by⁹

$$c_0 = e^{-\gamma \Delta t}; \quad c_1 = \frac{1 - c_0}{\gamma \Delta t}; \quad c_2 = \frac{1 - c_1}{\gamma \Delta t}. \quad (7)$$

δr_R and δv_R are small random displacements caused by the random force. As derived by Chandrasekhar¹⁰ the random displacements are distributed according to

$$\begin{aligned} w(\delta x_R) &= [2\pi\sigma_r\sigma_v\sqrt{1-c_{rv}^2}]^{-D} \\ &\times \prod_{\alpha=1}^D \exp\left\{-\frac{1}{2(1-c_{rv}^2)} \left[\left(\frac{\delta r_R^\alpha}{\sigma_r}\right)^2 + \left(\frac{\delta v_R^\alpha}{\sigma_v}\right)^2 \right. \right. \\ &\left. \left. - 2c_{rv} \left(\frac{\delta r_R^\alpha}{\sigma_r}\right) \left(\frac{\delta v_R^\alpha}{\sigma_v}\right) \right] \right\}, \end{aligned} \quad (8)$$

where $\delta x_R = \{\delta r_R, \delta v_R\}$ and α denotes the different components of the D -dimensional displacement vectors δr_R and δv_R . The variances σ_r and σ_v and the correlation coefficient c_{rv} are given by

$$\begin{aligned} \sigma_r^2 &= \Delta t \frac{k_B T}{m\gamma} [2 - (3 - 4e^{-\gamma \Delta t} + e^{-2\gamma \Delta t})/\gamma \Delta t], \\ \sigma_v^2 &= \frac{k_B T}{m} (1 - e^{-2\gamma \Delta t}), \\ c_{rv} \sigma_r \sigma_v &= \frac{k_B T}{m\gamma} (1 - e^{-\gamma \Delta t})^2. \end{aligned} \quad (9)$$

Applying Eq. (6) iteratively with random numbers drawn from the bivariate distribution (8) leads to a stochastic trajectory of arbitrary length. This procedure is usually called Brownian dynamics. Each trajectory generated with this algorithm has an associated probability that depends on the sequence of random displacements used to obtain the trajectory. The single step transition probability $p(x_\tau \rightarrow x_{\tau+1})$ is related to the random displacement δx_R by

$$p(x_\tau \rightarrow x_{\tau+1}) dx_{\tau+1} = w(\delta x_R) \left| \frac{\partial \delta x_R}{\partial x_{\tau+1}} \right| dx_{\tau+1}, \quad (10)$$

where δx_R can be calculated from Eq. (6) as a function of x_τ and $x_{\tau+1}$. The second factor on the right hand side of Eq. (10) is a Jacobian originating from the variable transformation from δx_R to $x_{\tau+1}$. For the integration algorithm (6) the Jacobian equals unity. By substituting L short-time transition probabilities $p(x_\tau \rightarrow x_{\tau+1})$ into Eq. (2) one obtains the probability of a transition path of length $\mathcal{T} = L\Delta t$.

Of course, in order to be compatible with the path action (2) the transition probability (10) has to preserve the canonical distribution. To demonstrate this preservation we first compare the probability $p(x \rightarrow y)$ to go from x to y in a time increment Δt with the probability to go back from y to x after reversing the momenta. An expansion in powers of Δt gives to first order in Δt

$$\frac{p(x \rightarrow y)}{p(\bar{y} \rightarrow \bar{x})} = e^{-\beta[H(y) - H(x)]}. \quad (11)$$

Here, \bar{x} and \bar{y} denote the phase space points obtained from x and y , respectively, by reversing the momenta, $\{r, v\} \rightarrow \{r, -v\}$. We note that for constant forces this result is exact. From this result, it follows that $p(x \rightarrow y)$ conserves the canonical distribution. That is,

$$\int dx e^{-\beta H(x)} p(x \rightarrow y) = e^{-\beta H(y)} \int dx p(\bar{y} \rightarrow \bar{x}) = e^{-\beta H(y)}, \quad (12)$$

where the second equality follows from the facts that the transition probability is normalized and that the Jacobian of the coordinate transformation from x to \bar{x} is unity.

III. SIMULATION METHODS

In this section, we introduce a new Monte-Carlo method to sample the distribution of paths efficiently. It consists of generating a new trial path from the current path and accepting it with a probability $P_{\text{acc}}^{\text{old} \rightarrow \text{new}}$ that satisfies the detailed balance condition

$$e^{-S_{AB}[\{x^{\text{old}}\}]} P_{\text{gen}}^{\text{old} \rightarrow \text{new}} P_{\text{acc}}^{\text{old} \rightarrow \text{new}} = e^{-S_{AB}[\{x^{\text{new}}\}]} P_{\text{gen}}^{\text{new} \rightarrow \text{old}} P_{\text{acc}}^{\text{new} \rightarrow \text{old}}, \quad (13)$$

where $P_{\text{gen}}^{\text{old} \rightarrow \text{new}}$ is the probability of generating the new path from the old one, and $P_{\text{acc}}^{\text{old} \rightarrow \text{new}}$ is the probability of accepting the new path. Similarly, $P_{\text{gen}}^{\text{new} \rightarrow \text{old}}$ and $P_{\text{acc}}^{\text{new} \rightarrow \text{old}}$ are the generation and acceptance probabilities for the reverse move, respectively. The corresponding Metropolis acceptance criterion for accepting the new path is then given by

$$P_{\text{acc}}^{\text{old} \rightarrow \text{new}} = \min \left[1, \frac{e^{-S_{AB}[\{x^{\text{new}}\}]} P_{\text{gen}}^{\text{new} \rightarrow \text{old}}}{e^{-S_{AB}[\{x^{\text{old}}\}]} P_{\text{gen}}^{\text{old} \rightarrow \text{new}}} \right]. \quad (14)$$

If the new path is rejected, the old one serves as the current path. In the following sections, we describe two procedures for generating new paths and derive the appropriate acceptance probabilities for the path action (2). Analogous formulas for the action (4) can be obtained by replacing the constraint function $h_B(x_L)$ by $\tilde{h}_B[\{x\}]$.

A. Shooting algorithm

Consider a path in phase space as depicted schematically in Fig. 1. One can create part of a new path by choosing a time slice τ at random and computing a Brownian dynamics trajectory starting from the phase space coordinates x_τ until one reaches time $\mathcal{T} = L\Delta t$. The new path consists of the time slices 0 to τ of the old path and the newly generated time slices $\tau+1$ to L . Due to the random displacements occurring in the Brownian dynamics algorithm, the new path will

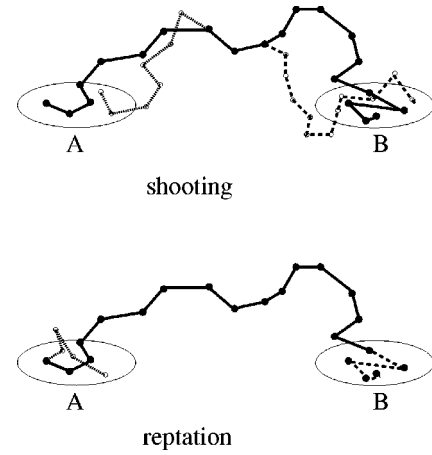


FIG. 1. Schematic representation of the shooting and the reptation sampling algorithm. In the shooting algorithm new paths are generated by selecting a time slice along a given path at random and shooting off a path in forward (dashed line) or backward (dotted line) direction. Reptation moves consist of deleting time slices from one side of the path and appending new time slices on the other side. Suitable acceptance criteria guarantee that paths are sampled according to their weight.

quickly diverge from the old path. The generating probability for the new trajectory starting at time slice τ is

$$P_{\text{gen}}^{\text{old} \rightarrow \text{new}} = \prod_{i=\tau}^{L-1} p(x_i^n \rightarrow x_{i+1}^n). \quad (15)$$

Because this product also appears exactly in the path probability $e^{-S_{AB}[\{x^n\}]}$ and the time slices $i \leq \tau$ remain unchanged, most of the factors in the acceptance probability (14) cancel and we obtain

$$P_{\text{acc}}^{\text{old} \rightarrow \text{new}} = h_B(x_L^n). \quad (16)$$

Any path beginning from an intermediate time slice is accepted provided the path eventually reaches region B.

This ‘‘shooting’’ procedure samples the time slices close to the initial region A very slowly, since paths initialized in A very rarely end in B. To remedy this problem, one also performs shooting backward in time. Again one randomly chooses a time slice τ , but now one reverses the momenta at that time slice and performs a regular Brownian dynamics simulation backwards in time until one reaches the first time slice $\tau=0$. Then the momenta are reversed at each time slice in the new path segment, so that the entire path evolves forward in time. Accordingly, the generating probability for a backward trajectory starting at time slice τ is

$$P_{\text{gen}}^{\text{old} \rightarrow \text{new}} = \prod_{i=0}^{\tau-1} p(\bar{x}_{i+1}^n \rightarrow \bar{x}_i^n), \quad (17)$$

where $\bar{x} = \{r, -v\}$ denotes the phase space point obtained from $x = \{r, v\}$ by reversing the momenta. When inserted into Eq. (14) one obtains

$$P_{\text{acc}}^{o \rightarrow n} = \min \left[1, \frac{e^{-\beta E(x_0^n)} h_A(x_0^n) h_B(x_L^n)}{e^{-\beta E(x_0^o)} h_A(x_0^o) h_B(x_L^o)} \right. \\ \left. \times \frac{\prod_{i=0}^{L-1} p(x_i^n \rightarrow x_{i+1}^n) \prod_{i=0}^{\tau-1} p(\bar{x}_{i+1}^o \rightarrow \bar{x}_i^o)}{\prod_{i=0}^{L-1} p(x_i^o \rightarrow x_{i+1}^o) \prod_{i=0}^{\tau-1} p(\bar{x}_{i+1}^n \rightarrow \bar{x}_i^n)} \right]. \quad (18)$$

Unlike the factors in the acceptance probability for the forward trajectory, the products in this equation do not cancel in general. However, for the Langevin equation in the limit of small time increment Δt , Eq. (11) is valid. Substituting Eq. (11) into Eq. (14), and using the fact that the time slices $i \geq \tau$ do not change, the resulting acceptance probability becomes simply

$$P_{\text{acc}}^{o \rightarrow n} = h_A(x_0^n). \quad (19)$$

This result implies that any new path which reaches region A at time $\tau=0$ is accepted.

In summary, the ‘‘shooting algorithm’’ chooses a random time slice τ and ‘‘shoots off’’ a trajectory either forward or backward in time. The new path is accepted if it ends in either the final or initial stable state, respectively. This method achieves linear scaling with path length and is therefore much more efficient than the dynamical, local and configurational bias methods described in Ref. 5. In using the algorithm, one imagines that there are only two accessible stable states separated by a barrier region. If there are additional nearby stable states, trajectories intended to span between regions A and B might instead become trapped in the additional metastable states. We will return to this issue when discussing the application of the path sampling method to cluster rearrangements.

B. Improving averages by reptation

In order to enhance the equilibration of paths one can perform ‘‘reptation’’ moves, in which time slices are removed from the beginning of the path and new slices are appended to the end of the path, or vice versa. (The term ‘‘reptation’’ was originally introduced by de Gennes¹¹ to describe the movement of a polymer in a dense melt. We use the same term here because of the analogy between polymers and transition paths.)

A move that deletes m time slices from the beginning of the path and appends m new time slices to the end of the path is performed by first shifting the last $L-m$ time slices of the old path such that $x_i^n = x_{i+m}^o$ for $i=0, \dots, L-m$. Then m new time slices are appended to the path by performing m Brownian dynamics steps beginning at x_{L-m}^n . Accordingly, the generating probability for the new path is given by

$$P_{\text{gen}}^{o \rightarrow n} = \prod_{i=L-m}^{L-1} p(x_i^n \rightarrow x_{i+1}^n). \quad (20)$$

where m is chosen randomly between 0 and L . To obtain the acceptance probability for the new path one has to consider the generation probability for the reverse move, which consists of deleting m time slices at the end of the path and appending new time slices on the other side. To perform such a move, one must first shift the path such that x_i^o

$= x_{i-m}^n$ for $i=m, \dots, L$. Then one calculates a backward trajectory of m steps starting from x_m^o . The probability to generate the path $\{x^o\}$ from $\{x^n\}$ is given by

$$P_{\text{gen}}^{n \rightarrow o} = \prod_{i=0}^{m-1} p(\bar{x}_{i+1}^o \rightarrow \bar{x}_i^o). \quad (21)$$

Provided the forward and the backward moves are attempted with the same probability, it follows from Eq. (14) that the new path $\{x^n\}$ is accepted with the probability

$$P_{\text{acc}}^{o \rightarrow n} = \min \left[1, \frac{e^{-\beta H(x_0^n)} h_A(x_0^n) h_B(x_L^n)}{e^{-\beta H(x_0^o)} h_A(x_0^o) h_B(x_L^o)} \right. \\ \left. \times \frac{\prod_{i=0}^{L-1} p(x_i^n \rightarrow x_{i+1}^n) \prod_{i=0}^{m-1} p(\bar{x}_{i+1}^o \rightarrow \bar{x}_i^o)}{\prod_{i=0}^{L-1} p(x_i^o \rightarrow x_{i+1}^o) \prod_{i=L-m}^{L-1} p(x_i^n \rightarrow x_{i+1}^n)} \right]. \quad (22)$$

Using Eq. (11) the acceptance probability reduces to

$$P_{\text{acc}}^{o \rightarrow n} = h_A(x_0^n) h_B(x_L^n). \quad (23)$$

For the backwards move, which deletes m time slices from the end of the path and appending new ones at the beginning of the path, the situation is completely symmetrical. The probability to accept a new path is therefore identical to Eq. (23).

Reptation obviously does not affect any time slice in which the system is on the barrier between A and B , so it cannot be used to sample completely new transition paths. It can be used to supplement the shooting algorithm. Whereas shooting moves the path in a transversal direction, reptation shifts the path back and forth in time.

C. Path quenching

From a transition path simulation one obtains a large set of paths connecting the initial and the final regions. Analysis is required to extract qualitative and quantitative path features from this set. For example, one might be interested in the following questions: How many typical reaction channels exist? Which transition states and metastable states are visited by the system on its way from the reactants to the products? What are the prominent characteristics of the reaction mechanism? Is it possible to describe the reaction by a small set of reaction coordinates? One way to answer such questions is to perform ‘‘path quenching.’’ In this method, we determine the most probable paths by computing the local minima of the action.

From the transition probability (10) it follows that at a given temperature $T = (k_B \beta)^{-1}$, the action (2) can be written as

$$S_{AB}[\{x\}] = \beta U_P[\{x\}] + C, \quad (24)$$

where C is a constant depending on the time increment Δt and the friction γ . The ‘‘path energy’’ $U_P[\{x\}]$, which has the dimension of energy, is a function of all path coordinates, but is independent of the temperature $k_B T$. $U_P[\{x\}]$ also contains the endpoint constraints that act as hard walls con-

fining the initial state x_0 and the final state x_L to the regions A and B , respectively. Accordingly, the weight of a given path can be expressed as

$$P[\{x\}] \propto e^{-\beta U_P[\{x\}]}, \quad (25)$$

which has the same form as a Boltzmann factor of a classical many body system.

Now, imagine the system is following a transition path at low temperature. According to Eq. (25) paths corresponding to a minimum of $U_P[\{x\}]$ are strongly favored. Thus, in a low temperature system, the paths simply fluctuate about a least action path. Typically, paths close to a least action path share the same basic properties. A least action path can therefore be regarded as a representative for an ensemble of similar paths.

In a complex system there might be several distinct low action paths connecting regions A and B . These paths correspond to the local minima of the action $S_{AB}[\{x\}]$ or, equivalently, of the path energy $U_P[\{x\}]$. The local minima can be found by a conjugate gradient method starting from different paths. This procedure partitions the whole path space into different basins of attractions around the local minima of the action-surface. As a result, one reduces the original large set of transition paths to a small set of least action paths, which can be easily examined and viewed. This procedure, similar in spirit to Stillinger and Weber's¹² quenching analysis, is most useful if the fluctuations around the minimum action paths are small. At low temperature, this condition is met, and the classification of paths by quenching is a practical way to explore the path ensemble.

D. Order parameters for the stable regions

In general, the initial and final stable regions A and B are characterized by the functions $h_A(x)$ and $h_B(x)$. Their specification coincides with a choice of an order parameter that distinguishes between the two stable regions. For ease in directing paths from one stable state to another, it is most convenient if the order parameter is low dimensional. Irrespective of convenience, it is required that the order parameter truly distinguishes. If a particular value of the order parameter is possible in both states A and B , a simulation will eventually produce paths that remain nearly always in only one of the stable regions. In other words, non-discriminating $h_A(x)$ and $h_B(x)$ will fail to produce transition paths.

In cases where the final and initial states are specific conformations of a many-particle system, a simple way to identify the stable states is through the mean square displacement δr^2 from that specific conformation,

$$\delta r^2 = \sum_{i=1}^N (\mathbf{U}r_i - r_i^0)^2. \quad (26)$$

Here, N is the number of particles or atoms and r_i^0 is the position of particle i in the stable state conformation. It is assumed that both r and r^0 have their center of mass in the origin. \mathbf{U} is a rotation matrix chosen to minimize the mean square displacement. This minimum value δr_{\min}^2 is used to determine whether a configuration is in the stable state. The functions $h_A(x_\tau)$ and $h_B(x_\tau)$ can then be written as

$$h_{A,B}(x) = \begin{cases} 1, & \text{if } \delta r_{\min}^2 < c, \\ 0, & \text{if } \delta r_{\min}^2 > c. \end{cases} \quad (27)$$

The constant c must be chosen such that regions A and B are large enough to accommodate the equilibrium fluctuations of the system around the respective potential energy minima.

This approach is limited to stable states that can be characterized by proximity to a single conformation.

IV. CALCULATING RATE CONSTANTS

In our previous work⁵ we have shown how the path sampling method can be used for the calculation of rate constants. Here, we first quickly restate the pertinent result from that paper, and then we show how the method can be improved by using action (4) instead of action (2).

The fluctuation-dissipation theorem relates the rate constant for a transition between stable states to microscopic correlation functions (see, for example, Ref. 13):

$$k(t) \equiv \frac{\langle h_A(x(0)) \dot{h}_B(x(t)) \rangle}{\langle h_A(x(0)) \rangle} \approx k_{A \rightarrow B} \exp(-t/t_{\text{rxn}}), \quad (28)$$

where h_A and h_B are the characteristic functions for the stable states as defined in Eq. (3), the dot denotes the time derivative, and $t_{\text{rxn}} = (k_{A \rightarrow B} + k_{B \rightarrow A})^{-1}$ is the reaction time with $k_{A \rightarrow B}$ and $k_{B \rightarrow A}$ as the forward and backward reaction rate constants, respectively. The brackets $\langle \dots \rangle$ indicate ensemble averages. The correlation function in Eq. (28) is the time derivative of the probability for observing the system in region B at time t provided it was in region A at time $\tau = 0$. For barriers large compared to $k_B T$, $k(t)$ reaches a plateau after a molecular relaxation time t_{mol} which is assumed to be much shorter than the reaction time, $t_{\text{mol}} \ll t_{\text{rxn}}$. Because of this separation of time scales, $\exp(-t/t_{\text{rxn}}) \approx 1$ in this time regime, and the plateau value of $k(t)$ is equal to the phenomenological rate constant $k_{A \rightarrow B}$.

To calculate $k(t)$ in the path sampling method, we consider discrete times and rewrite Eq. (28) as

$$k(\tau) = \frac{\langle h_A \dot{h}_B(x_\tau) \rangle}{\langle h_A \rangle} = \frac{\langle h_A \dot{h}_B(x_\tau) \rangle}{\langle h_A h_B(x_L) \rangle} \times \frac{\langle h_A h_B(x_L) \rangle}{\langle h_A \rangle} \equiv \nu(\tau) \times P. \quad (29)$$

Here, and in the following, we drop the argument of $h_A(x_0)$ to simplify the notation. It is, however, understood that h_A is always a function of x_0 , the first time slice of the transition path.

In Eq. (29) we have factorized $k(\tau)$ into a frequency factor $\nu(\tau) \equiv \langle h_A \dot{h}_B(x_\tau) \rangle / \langle h_A h_B(x_L) \rangle$ and a probability factor $P \equiv \langle h_A h_B(x_L) \rangle / \langle h_A \rangle$. To calculate the frequency factor $\nu(\tau)$ in the transition path ensemble, we recast the definition of $\nu(\tau)$ as

$$\begin{aligned} \nu(\tau) &= \frac{\langle h_A \dot{h}_B(x_\tau) \tilde{h}_B[\{x\}] \rangle}{\langle h_A \tilde{h}_B[\{x\}] \rangle} \times \frac{\langle h_A \tilde{h}_B[\{x\}] \rangle}{\langle h_A h_B(x_L) \rangle} \\ &\equiv \frac{\langle \dot{h}_B(x_\tau) \rangle_{AB}}{\langle h_B(x_L) \rangle_{AB}}, \end{aligned} \quad (30)$$

where we have used the fact that $\tilde{h}_B[\{x\}]$ is zero only if $h_B(x_\tau)$ vanishes for all τ from 0 to L . The numerator $\langle \dot{h}_B(x_\tau) \rangle_{AB}$ is the path average of $\dot{h}_B(x_\tau)$ with respect to the action (4). With this same notation, the denominator in the last equality of Eq. (30) is the average probability for the last time slice to lie in region B provided that the path visits B at least once in the time interval $[0, L]$. If the transition from A to B is a rare event and region B is suitably defined, $\langle h_B(x_L) \rangle_{AB} \approx 1$. The second factor in Eq. (29), the probability factor $P \equiv \langle h_A h_B(x_L) \rangle / \langle h_A \rangle$, is the probability of the last time slice to be in region B provided the path started in region A at $\tau=0$.

To determine $k(\tau)$, one must determine both $\nu(\tau)$ and P . The first of these ratios may be obtained from a single path sampling simulation. Since $\nu(\tau)$ is the only term in Eq. (29) depending on the time index τ , it is expected to reach a plateau value after the molecular time t_{mol} .^{2,13} This plateau value, ν_{pl} , is to be used in the calculation of the rate constant $k_{A \rightarrow B}$. In fact, we can use the occurrence of a plateau as a criterion to determine whether the transition path is sufficiently long, i.e., whether the number of time slices is sufficient to capture the most likely transition paths.

To calculate the probability factor, P , one may employ umbrella sampling,^{14,15} as we discussed in Ref. 5. The phase space is divided into several slightly overlapping regions, or ‘‘windows,’’ B_i defined by $\lambda_i^{\text{min}} < \lambda < \lambda_i^{\text{max}}$, where λ is a suitable stable state order parameter. Then, a series of path simulations is performed for the same initial region A but with varying final regions B_i . For every simulation one constructs a histogram of the order parameter λ at the endpoint of the path. Matching the histograms of each window results in a ‘‘master histogram’’ $f(\lambda)$ representing the entire probability distribution of finding the order parameter λ . The probability factor P is then found by integration

$$P = \frac{\langle h_A h_B(x_L) \rangle}{\langle h_A \rangle} = \frac{\int_B f(\lambda) d\lambda}{\int f(\lambda) d\lambda}, \quad (31)$$

where \int_B denotes an integration over all values of λ belonging to the final region B .

In summary, one divides the calculation of $k(t)$ into two parts by using the factorization (29). The first factor, $\nu(\tau)$, contains the time dependence of $k(\tau)$ and can be calculated from a single transition path simulation. Furthermore, by looking for a plateau in $\nu(\tau)$ one can check if the path is long enough for the calculation of a rate constant. The second step in the determination of the rate constant consists of calculating $\langle h_A h_B(x_L) \rangle / \langle h_A \rangle$. This calculation can be done by using free energy estimation methods, like umbrella sampling. Since it usually involves several independent path simulations, part two of the procedure is the computationally more expensive one.

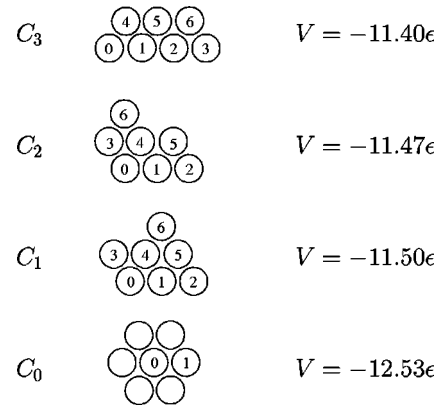


FIG. 2. The stable configurations of the cluster and their respective energies. The numbers in the disks are used to detail the position of a particle in the cluster.

V. RESULTS ON THE CLUSTER REARRANGEMENTS

A. The system

We illustrate the transition path sampling method on a cluster of seven particles in two dimensions. The particles have mass m and interact via the Lennard-Jones potential

$$V = \sum_{i < j} 4\epsilon \left[\left(\frac{\sigma}{r_{ij}} \right)^{12} - \left(\frac{\sigma}{r_{ij}} \right)^6 \right], \quad (32)$$

where $r_{ij} = |\mathbf{r}_i - \mathbf{r}_j|$ is the distance between particle i and particle j . We use reduced Lennard-Jones units throughout, i.e., distances are measured in units of σ , energies in units of ϵ , and time in units of $\tau_0 = (m\sigma^2/\epsilon)^{1/2}$. Accordingly, reaction rate constants k and the friction coefficient γ are given in units of τ_0^{-1} . The time evolution of the cluster is governed by the Langevin equation. At low temperatures, the cluster fluctuates around its potential energy minimum. From time to time, the particle originally in the middle of the cluster escapes to its surface. To elucidate this mechanism, one might try to perform a conventional straightforward Brownian dynamics simulation employing, for example, the integration algorithm (6). However, within time scales accessible to computer simulations very few transitions occur at low temperatures. Thus, for cold clusters, straightforward simulation is not suitable for the study of rearrangement processes. The system therefore provides an excellent illustrative case for the application of transition path sampling. In the next section we first explore the qualitative properties of structural transitions by path quenching. Then we compute transition rate constants for some selected processes.

B. Path quenching

To gain some insight into the cluster rearrangements, we determined least action paths for the migration of a particle from the center of the cluster to its surface. For this purpose, we performed a path simulation of length $L=400$ at $k_B T = 0.1\epsilon$, using both shooting and reptation. The time increment was $\Delta t = 0.05\tau_0$ and the friction $\gamma = 4.0/\tau_0$. At time slice $\tau=0$, the central particle is required to be closer than $R=0.15\sigma$ to the center of mass of the cluster, whereas at time slice $\tau=L$ a different particle is constrained to occupy

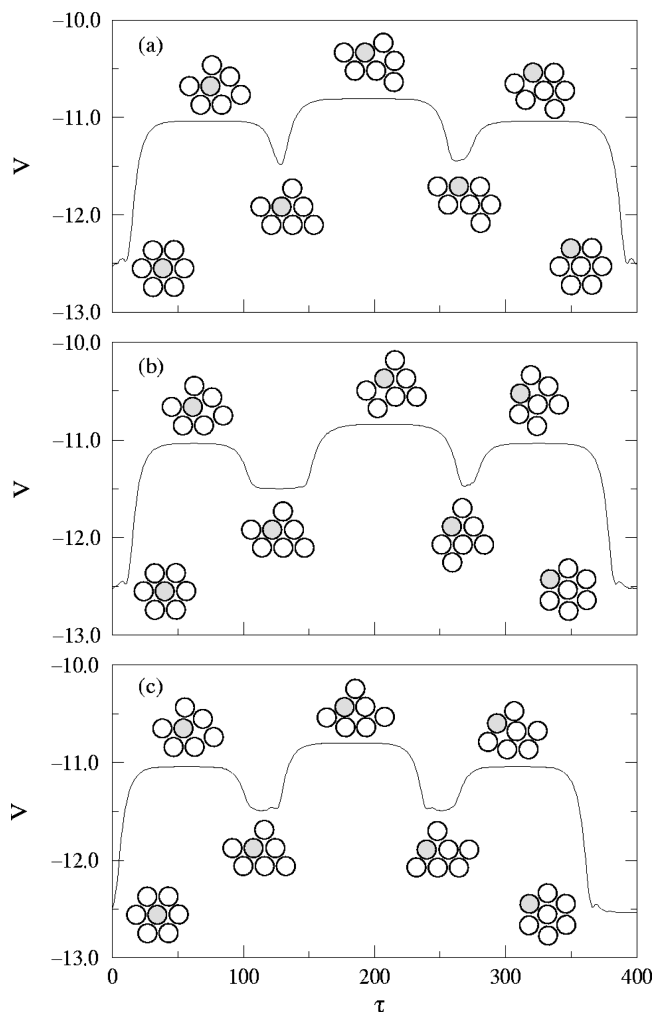


FIG. 3. Profiles of the potential energy for three different paths obtained by path quenching at $k_B T = 0.1\epsilon$ and $\gamma = 4.0/\tau_0$. The initial paths for the quenching procedure were obtained from a transition path simulation where the particle initially in the middle of the cluster is required to be on its surface at the end of the process. The configurations depicted below the curves are the stable states visited during the transition and the configurations above the curves are the transition states. The shaded particle is the particle initially in the center of the cluster.

this position. These boundary conditions force the path to start from and to end in a configuration close to the global minimum of the potential energy, which we denote by C_0 . Accordingly, the other local minima of the potential energy are referred to as C_1 , C_2 , C_3 , where the subscript labels the minima according to their energy. The four stable (metastable) cluster configurations are depicted in Fig. 2. Later, we will need to specify also the position of particles in the stable configurations. For this purpose we use an additional index as shown in the figure.

During the path simulation, paths were periodically saved and were used later as initial paths for the quenching procedure. To search for the minimum of the action $S_{AB}[\{x\}]$ we employed a conjugate gradient method.¹⁶ Within this method not only the action $S_{AB}[\{x\}]$ but also its gradient $\nabla S_{AB}[\{x\}]$ needs to be evaluated. Typical energy profiles of low action paths obtained from this procedure are shown in Fig. 3. These energy profiles are smooth because the random fluctuations around the most probable path have

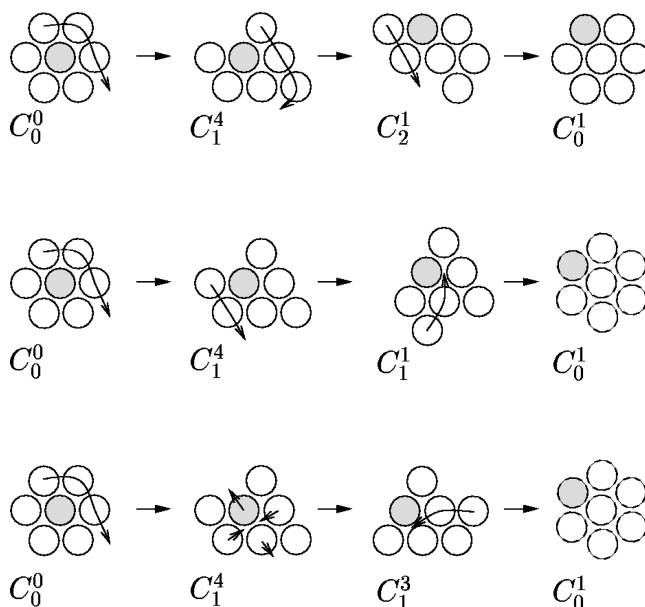


FIG. 4. The three predominant pathways for the migration of a particle from the center of the cluster to its surface. The superscripts denote the position of the tagged (shaded) particle according to the particle positions defined in Fig. 2.

been eliminated by the quenching process. The configurations of the cluster at the local minima of the potential energy profile are shown below the curves. These configurations correspond to the stable states shown in Fig. 2. Evidently, the system typically visits different metastable states on its way from the initial to the final state. The transition state configurations shown above the curves in Fig. 3 are obtained by determining the local maxima of the potential energy profile.

To characterize the stable states further we specify the position of the particle initially in the center of the cluster. Henceforth, this particle is called the tagged particle and shown as shaded in the figures. Thus, the transition starts in C_0^0 and ends in C_0^1 , where the superscript denotes the position of the tagged particle as defined in Fig. 2. From the transitions observed in the quenched paths three main mechanisms for the reaction from C_0^0 to C_0^1 can be identified (see Fig. 4). We note that the limited duration of the path does not allow for more transitions between different states C_i before the system finally reaches C_0^1 . For paths without time limit, however, one expects several transitions separated by long sojourns in the metastable states.

Another way to filter out the main characteristics of a noisy pathway is to determine the potential energy minimum at each time slice along the path. In other words, one quenches the cluster configuration at each time slice using a conjugate gradient or a steepest descent method obtaining a local minimum of the potential energy. From this procedure the same pathways for the process $C_0^0 \rightarrow C_0^1$ emerge. While computationally less expensive than path quenching, this approach does not yield any rigorous information about the transition states visited during the reaction. Miller and Wales¹⁷ have used quenched cluster configurations along with the conventional molecular dynamics to make estimates

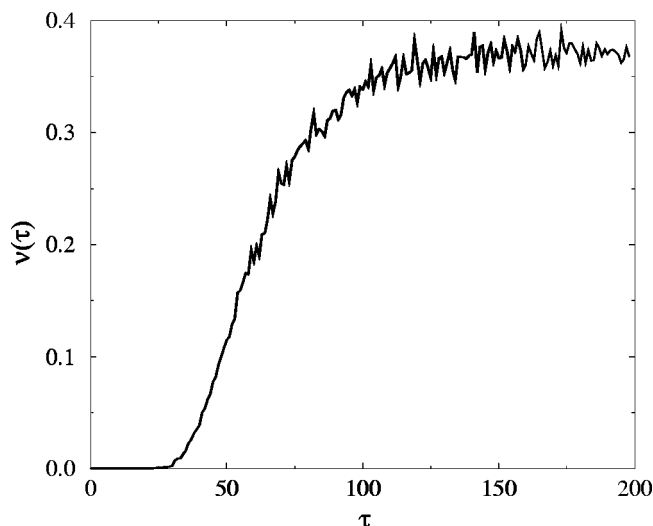


FIG. 5. Frequency factor $\nu(\tau)$ as a function of τ for the transition $C_0^0 \rightarrow C_1^4$. The reciprocal temperature was $\beta=20/\epsilon$, the friction coefficient was $\gamma=1/\tau_0$, and the time increment was $\Delta t=0.02\tau_0$.

of isomerization rate constants for a 7-atom Lennard-Jones cluster in three dimensions over a limited energy range. In contrast, path sampling and path quenching could provide reliable results over a wide energy range.

C. Rate constants

In a typical transition from C_0^0 to C_0^1 , the cluster visits a varying number of metastable states before it finally reaches the stable state C_0^1 . At low temperatures the residence time of the system in these metastable states is much larger than the molecular time scale t_{mol} . Nevertheless, there is a well defined reaction rate constant for the process $C_0^0 \rightarrow C_0^1$, because the typical lifetime of the stable configuration C_0 is much larger than the lifetimes of the intermediate states C_1 , C_2 , and C_3 . However, in this case the path length needed to reach the plateau region of $k(t)$ exceeds the path length tractable in transition path simulations. The solution of this problem consists in splitting up the whole process into subprocesses comprising only single transitions between the potential energy minima. Due to the long residence time in the minima subsequent transitions can be regarded as uncor-

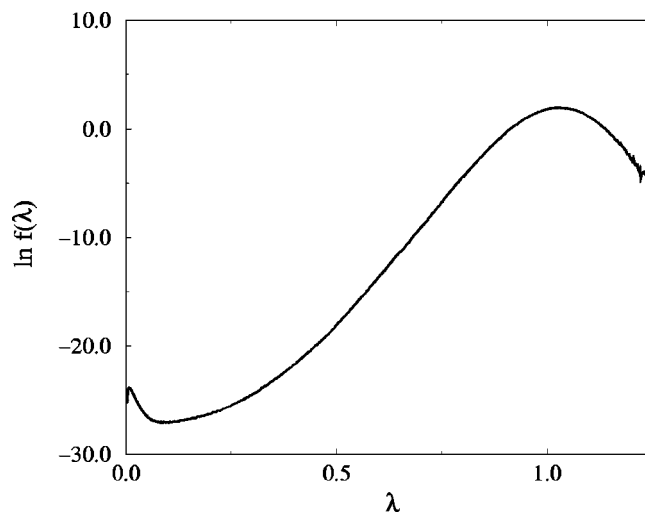


FIG. 6. Logarithm of the probability $f(\lambda)$ for the endpoint of the path to have a certain value of $\lambda \equiv \delta r^2$ for the transition $C_0^0 \rightarrow C_1^4$. The reciprocal temperature was $\beta=20/\epsilon$, the friction coefficient was $\gamma=1/\tau_0$, and the time increment was $\Delta t=0.02\tau_0$.

related. This fact allows us to determine the transition rate for the whole process from the reaction rate constants of single transitions.

Of all the possible reactions $C_0^0 \rightarrow C_0^1$, we chose the three most common, depicted in Fig. 4. We simulated all intermediate transitions separately, and for each, we sampled paths consisting of 200 time steps and calculated the frequency factor, $\nu(\tau)$, and the probability factor, P . The reciprocal temperature was $\beta=20/\epsilon$, the friction coefficient was $\gamma=1/\tau_0$, and the time increment was $\Delta t=0.02\tau_0$. The maximum mean square displacement from the potential energy minima was $c=0.1\sigma^2$. The umbrella sampling windows used in the determination of P were chosen such that in the histograms, the low side frequency was minimal 10% of the high side. This resulted in typically 10 to 12 windows. A simulation consisted of 1.5×10^6 shooting and 1×10^6 reptation attempts. The acceptance ratio ranged from a few percent to above 90% depending on the final region.

As an example, the frequency factor for the reaction $C_0^0 \rightarrow C_1^4$ is shown in Fig. 5. Figure 6 shows the logarithm of the probability for the endpoint to have a certain value for δr^2 as obtained by umbrella sampling for the same transition. The values of the rate constants for all subprocesses

TABLE I. Results of the path simulations for the subprocesses of the transitions shown in Fig. 4. The first column specifies the subprocess. For all the simulations the path length was $L=200$, the reciprocal temperature was $\beta=20/\epsilon$, the friction coefficient was $\gamma=1/\tau_0$, and the time increment was $\Delta t=0.02\tau_0$.

Reaction	V_A/ϵ	V_B/ϵ	V_{TS}/ϵ	$k\tau_0$	$\nu_{\text{pl}}\tau_0$	P
$C_0^0 \rightarrow C_1^4$	-12.53	-11.50	-11.037	3.50×10^{-13}	0.37	9.46×10^{-13}
$C_1^4 \rightarrow C_0^0$	-11.50	-12.53	-11.037	7.25×10^{-4}	0.37	1.96×10^{-3}
$C_0^1 \rightarrow C_2^1$	-12.53	-11.47	-11.040	2.77×10^{-13}	0.40	7.03×10^{-13}
$C_2^1 \rightarrow C_0^1$	-11.47	-12.53	-11.040	1.38×10^{-3}	0.40	3.47×10^{-3}
$C_1^4 \rightarrow C_2^1$	-11.50	-11.47	-10.807	5.30×10^{-7}	0.39	1.36×10^{-6}
$C_2^1 \rightarrow C_1^4$	-11.47	-11.50	-10.807	1.39×10^{-6}	0.39	2.72×10^{-6}
$C_1^4 \rightarrow C_1^1$	-11.50	-11.50	-10.841	1.20×10^{-6}	0.40	2.80×10^{-6}
$C_1^4 \rightarrow C_1^3$	-11.50	-11.50	-10.799	5.80×10^{-7}	0.35	1.65×10^{-6}

together with the energies of the corresponding stable states and transition states are summarized in Table I. Obviously, the transition rate is very low for the transitions with the highest barrier. Therefore, the rate determining step for the whole migration of a particle from the center of the cluster to its surface is the transition from C_0 to a metastable state. The transitions between neighboring metastable states and to the final stable state are comparatively fast. Whereas the plateau value ν_{pl} of ν varies only slightly between the different subprocesses, the probability factor P varies drastically determining the order of magnitude of the transition rate constant.

In order to check the validity of the rate constant calculation, we also studied the reverse reaction $C_1^4 \rightarrow C_0^0$. For a backward reaction the reactive flux $\nu(\tau)$ is the same as for the forward one. The probability to end in the stable state C_0^0 after L steps, when starting in the metastable state C_1^4 is $P = 0.00196$. This is much higher than the forward rate because the C_0^0 is the more stable state. The logarithm of the ratio between the forward and the backward rate constants, k_f/k_b , is equal to the free energy difference between the stable and the metastable state. For this particular reaction the free energy difference is

$$\beta\Delta F = \beta F_{C_0} - \beta F_{C_1} = \log(k_f/k_b) = -21.45.$$

The same free energy difference can be estimated by assuming the cluster is a collection of harmonic oscillators at the temperature under consideration. The potential energy contribution is simply given by the potential energy difference of the minima, $\Delta V = V_{C_0} - V_{C_1} = -1.03$. The entropy difference can be estimated by the frequencies ω of the harmonic oscillators in the stable states

$$\Delta S = S_{C_0} - S_{C_1} = \log \frac{\prod_{i=1}^{DN-3} \omega_i^{C_0}}{\prod_{i=1}^{DN-3} \omega_i^{C_1}}, \quad (33)$$

where we have eliminated the vanishing frequencies associated with the translation and rotation of the cluster as a whole. The frequencies ω_i are determined by diagonalizing the matrix of the force constants in the stable states. Because of translational and rotational invariance, three eigenvalues will be zero (in two dimensions). In the stable or metastable states all the other eigenvalues will be positive. The entropy difference is $\Delta S = S_{C_0} - S_{C_1} = 1.20$. The free energy difference is then $\beta\Delta F = \beta F_{C_0} - \beta F_{C_1} = \beta\Delta E - \Delta S = -21.80$. This number is close to the value obtained from the rate constant calculation, suggesting the validity of the transition path sampling method.

D. Efficiency and scaling

Our goal is to create an ensemble of independent paths in an efficient way. The efficiency of a method is partly determined by the correlation between paths as a function of the number n_c of simulation cycles. In this section, we examine the scaling behavior of the efficiency of the shooting and reptation method with the path length L . For this purpose we introduce the following correlation function

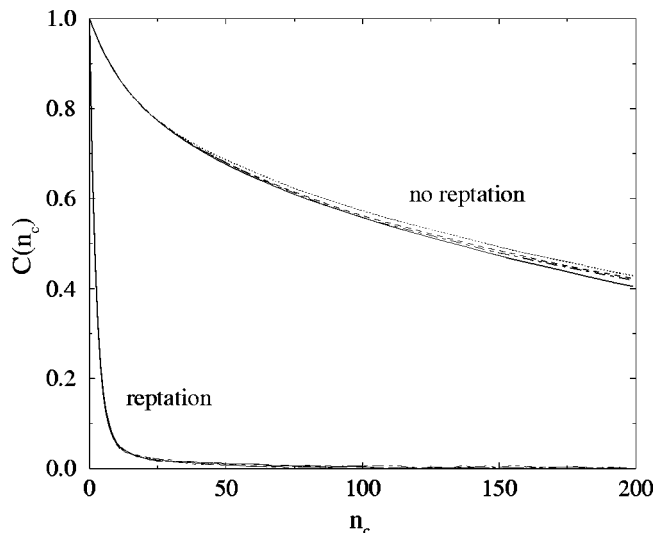


FIG. 7. Correlation function $C(n_c)$ as a function of the number n_c of simulation cycles for the subprocess $C_0^0 \rightarrow C_1^4$ at $\beta = 20/\epsilon$ and $\gamma = 1.0/\tau_0$ with and without reptation moves. The paths consisted of $L = 100, 200, 400$ and 800 time slices and the time increment Δt was adjusted to obtain the same total duration $\Delta t L = 4.0\tau_0$. As can be inferred from the figure using reptation moves speeds up the simulations considerably. Since the curves do not depend on the path length L and a computer time proportional to the length of the path is necessary to perform one cycle of the simulation, the computational effort of the simulation scales linearly with the length of the path L .

$$C(n_c) = \frac{\langle \delta h_B(x_{L/2}^0) \delta h_B(x_{L/2}^{n_c}) \rangle_{AB}}{\langle (\delta h_B(x_{L/2}^0))^2 \rangle_{AB}}. \quad (34)$$

Here, $\delta h_B(x_\tau^i) = h_B(x_\tau^i) - \langle h_B(x_\tau) \rangle_{AB}$ is the deviation of the characteristic function $h_B(x_\tau)$ from its ensemble average at simulation cycle i .

We performed simulations of the subprocess $C_0^0 \rightarrow C_1^4$ for paths consisting of $L = 100, 200, 400$ and 800 time slices. In order to study the same process spanning the total time $L\Delta t$ we have to scale the time increment Δt accordingly. The time increments were $\Delta t/\tau_0 = 0.04, 0.02, 0.01, 0.005$, respectively. The reciprocal temperature was again $\beta = 20/\epsilon$, and the friction coefficient was $\gamma = 1/\tau_0$. The maximum mean square displacement from the potential energy minima was $c = 0.1\sigma^2$.

A simulation cycle consisted of 1 shooting and 1 reptation attempt. To study the effect of the reptation algorithm we also performed a series of path simulations without reptation. Figure 7 shows the correlation functions $C(n_c)$ for the different path lengths with and without reptation. Clearly, the correlation time between paths does not change with path length. This means that the required computer time to sample independent path scales linearly with L , because for every path L integration steps have to be performed. This is a great improvement over the dynamical, local and configurational bias schemes, used in Refs. 5 and 7, which scale as L^2 , L^3 and $L^{1.5}$, respectively.

As is also clear from Fig. 7, the reptation algorithm has a huge effect on the correlation time. Reptation quickly averages out correlations by shifting the path in time. The shooting algorithm should therefore always be used in combination with reptation.

VI. CONCLUSION

In summary, we have developed an efficient algorithm for the sampling of stochastic transition paths. As an illustration, we have applied the method to a 7-particle Lennard-Jones cluster in two dimensions. Though this system is of only moderate complexity (14 degrees of freedom) a remarkable variety of different transition pathways has been found. By quenching paths with respect to their associated path action we have identified the relevant reaction mechanisms and localized the transition states.

As estimated from the decay of correlations functions, the numerical effort necessary to perform path simulations scales linearly with the length L of the paths. Hence, the simulation of realistic reactions in condensed matter systems, e.g., chemical reactions in solution, becomes feasible. In contrast to the sampling methods developed in Ref. 5, the efficiency of the algorithms does not degrade for low friction constants. The Newtonian limit can therefore be approached with the shooting and reptation algorithm. In fact, very similar algorithms can be used to sample deterministic transition paths.⁸

ACKNOWLEDGMENTS

We thank Felix Csajka for useful discussions and Phillip Geissler for a critical reading of the manuscript. This work was initiated with support from the National Science Foundation and completed with support from the Department of Energy through the Chemical Sciences Division of Lawrence

Berkeley National Laboratory. The calculations reported in this work were partly done on the Cray T3E at Lawrence Berkeley National Laboratory. C. Dellago gratefully acknowledges support from the Austrian Fonds zur Förderung der wissenschaftlichen Forschung Grants No. J01302-PHY and J1548-PHY.

¹C. H. Bennett, in *Algorithms for Chemical Computations*, ACS Symp. Ser. No. 46, ed. R. E. Christofferson (American Chemical Society, Washington, D. C., 1977), p. 63.

²D. Chandler, *J. Chem. Phys.* **68**, 2959 (1978).

³J. Keck, *J. Chem. Phys.* **32**, 1035 (1960).

⁴J. B. Anderson, *J. Chem. Phys.* **58**, 4684 (1973).

⁵C. Dellago, P. Bolhuis, F. S. Csajka, and D. Chandler, *J. Chem. Phys.* **108**, 1964 (1998).

⁶L. R. Pratt, *J. Chem. Phys.* **85**, 5045 (1986).

⁷F. S. Csajka and D. Chandler, *J. Chem. Phys.* (to be published).

⁸P. G. Bolhuis, C. Dellago, and D. Chandler, *Faraday Discuss.* **110** (in press, 1998).

⁹M. P. Allen and D. J. Tildesley, *Computer Simulation of Liquids* (Clarendon, Oxford, 1987).

¹⁰S. Chandrasekhar, *Rev. Mod. Phys.* **15**, 1 (1943).

¹¹P. de Gennes, *J. Chem. Phys.* **55**, 572 (1971).

¹²F. H. Stillinger and T. A. Weber, *Science* **225**, 983 (1984); **28**, 2408 (1983).

¹³D. Chandler, *Introduction to Modern Statistical Mechanics* (Oxford University Press, New York, 1987).

¹⁴G. M. Torrie and J. P. Valleau, *J. Comput. Phys.* **23**, 187 (1977).

¹⁵D. Frenkel and B. Smit, *Understanding Molecular Simulation* (Academic, San Diego, 1996).

¹⁶W. H. Press, S. A. Teukolsky, W. T. Vetterling, and B. P. Flannery, *Numerical Recipes in C*, 2nd ed. (Cambridge University Press, Cambridge, 1992).

¹⁷M. A. Miller and D. J. Wales, *J. Chem. Phys.* **107**, 8568 (1997).